

The Early Ultraviolet Evolution of the ONeMg Nova V382 Velorum 1999

Steven N. Shore

Dept. of Physics and Astronomy, Indiana University South Bend, 1700 Mishawaka Ave, South Bend, IN 46634-7111; Osservatorio Astrofisico di Arcetri, 5 Largo E. Fermi, I-50125 Firenze, Italy; Department of Physics, University of Pisa, Via Buonarroti 2, Pisa, 56100 Italy

`sshore@paladin.iusb.edu`

Greg Schwarz

Steward Observatory, University of Arizona, Tucson, AZ 85721

`gschwarz@as.arizona.edu`

Howard E. Bond and Ronald A. Downes

Space Telescope Science Institute, 3700 San Martin Drive, Baltimore, MD 21218

`bond@stsci.edu` and `downes@stsci.edu`

Sumner Starrfield

Dept. of Physics and Astronomy, Arizona State University, Tempe, AZ 85287-1504

`starrfield@asu.edu`

A. Evans

Dept. of Physics and Astronomy, Keele University, UK

`ae@astro.keeple.ac.uk`

Robert D. Gehrz

Department of Astronomy, University of Minnesota, 116 Church Street, SE, Minneapolis, MN 55455

`gehrz@hal.astro.umn.edu`

Peter H. Hauschildt

Hamburger Landsternwarte, Gojenbergweg 112, 21029 Hamburg, Germany

`peter.hauschildt@hs.uni-hamburg.de`

Joachim Krautter

Landessternwarte Heidelberg, Germany

`j.krautter@lsw.uni-heidelberg.de`

Charles E. Woodward

Department of Astronomy, University of Minnesota, 116 Church Street, SE, Minneapolis, MN 55455

`chelsea@astro.umn.edu`

ABSTRACT

DRAFT 26/11/02

We present a multiwavelength study of the ONeMg Galactic nova V382 Velorum 1999 using HST/STIS¹ and FUSE ultraviolet spectra and comparisons with published groundbased optical spectra. We find a close match to the basic phenomenology of another well-studied ONeMg nova, V1974 Cygni (Nova Cygni 1992), in particular to the spectral development through the start of the nebular phase. Following an “iron curtain” phase, the nova proceeded through a stage of P Cygni line profiles on all important resonance lines, as in many ONeMg novae and unlike the CO class. Emergent emission lines displayed considerable structure, as seen in V1974 Cyg, indicating fragmentation of the ejecta at the earliest stages of the outburst. Analysis and modeling of our ultraviolet spectra suggest that $4 - 5 \times 10^{-4} M_{\odot}$ of material was ejected and that the distance to the nova is $\simeq 2.5$ kpc. Relative to solar values, we find the following abundances: He = 1.0, C = 0.6 ± 0.3 , N = 17 ± 4 , O = 3.4 ± 0.3 , Ne = 17 ± 3 , Mg = 2.6 ± 0.1 , Al = 21 ± 2 , and Si = 0.5 ± 0.3 . Finally, we briefly draw comparisons with Nova LMC 2000, another ONeMg nova, for which similar data were obtained with HST and FUSE.

Subject headings: stars: individual: V382 Vel - novae, cataclysmic variables - ultraviolet: stars

¹Based on observations made with the NASA/ESA Hubble Space Telescope, obtained at the Space Telescope Science Institute, which is operated by Associated Universities for Research in Astronomy, Inc., under NASA contract 5-26555. These observations are associated with proposals for proposal GO 8540 and GO 8671. Also based on observations made with the NASA-CNES-CSA Far Ultraviolet Spectroscopic Explorer. FUSE is operated for NASA by the Johns Hopkins University under NASA contract NAS5-32985.

1. Introduction

Nova Velorum 1999 (V382 Vel) was discovered in outburst by P. Williams, and independently by C. Gilmore, on 1999 May 20.6 UT (Lee et al. 1999). It reached a maximum visual magnitude of $V = 2.6$ (Steiner, Campos, & Cieslinski 1999) after a few days of rise, making it among the brightest novae of the 20th century. Its decline showed $t_2 = 4$ days and $t_3 = 10$ days (Della Valle, Pasquini, & Williams 1999) marking it as a “fast” nova in the nomenclature introduced by Payne-Gaposchkin (1957) (t_2 and t_3 are the times after maximum for declines of two and three magnitudes, respectively). Platais et al. (2000) have determined a preoutburst mean V magnitude of $16.^m6$ and a mean B-V of $0.^m14$; a pre-outburst B magnitude of 16.4 was reported (Steiner, Campos, & Cieslinski 1999). Early optical spectroscopic observations displayed iron emission associated with the optically thick phase of a relatively massive ejection, although He I emission was reported relatively early (2 June, Hidayat et al. 1999). The first optical spectra, within two days of the first report, showed P Cyg absorption components on the Balmer lines (Lee et al. 1999). The report of very early [O III] emission was later corrected, identifying the emission as Fe II. Infrared observations (Woodward, Wooden, Pina, & Fisher 1999) detected the [Ne II] 12.8μ emission line characteristic of the “neon nova” group and subsequently V382 Vel has been recognized as an ONeMg nova.

V382 Vel displayed comparable optical phenomenology to the well studied the ONeMg nova V1974 Cygni (*e.g.* Shore et al. 1993, 1994; Shore 2002) and, as we will show here, its ultraviolet spectrum developed along similar lines. We are therefore able to make some interesting comparisons despite being unable to follow V382 Vel with the dedicated instrumentation used in our earlier investigations. In this paper, we will show that much of what we have learned about the physics of the early nova outburst from the detailed study of a single ONeMg nova, V1974 Cyg, is robust: the resemblance between these outbursts is striking and an important observational constraint on any model for the nova phenomenon.

2. Observations

Optical observations have been described by Della Valle et al. (2002). The ultraviolet (UV) observations reported here were obtained under a Director’s Discretionary target of opportunity program (GO 8540) with the *Space Telescope Imaging Spectrograph* (STIS) on board the *Hubble Space Telescope* (HST) in three epochs using the E140M and E230M gratings. Additional spectra were obtained with the *Far Ultraviolet Spectrographic Explorer* (FUSE) satellite on a galactic nova target of opportunity program at three epochs during 2000 using the large aperture in both the SiC and LiF channels. These observations were not accompanied by STIS spectra and were well into the optically thin stage. The last spectrum contains significant atmospheric emission and has not been used in this study. The log of observations is given in Table 1.

All spectra have been reduced using standard procedures for both STIS and FUSE and with

software we have previously developed to analyze UV spectra of novae. For consistency, we have attempted to duplicate previous analyses. Since the FUSE spectra were taken with the large science aperture, some shifting was required for wavelength assignments: the STIS and FUSE spectra were cross correlated in wavelength using the N I multiplet at 1199Å. The individual STIS spectra were registered using several interstellar absorption features, in particular the C II 1334Å, Al II 1671Å, and Mg II 2800Å doublets. The largest wavelength shift seen in the STIS data is 18 km s⁻¹, while the FUSE spectra were displaced by +40 km s⁻¹ from the STIS data. After correction, the individual line profiles were compared in velocity using the Morton (1991) and NIST Atomic Spectra Database (ASD).²

3. Temporal Development of V382 Vel within the First 16 Months

3.1. Spectral Development

The gallery of merged binned (1Å resolution) spectra is shown in Figs. 1, 2, and 3, and the high resolution data are displayed for the 1200-1720Å region in Figs. 4, 5, and 6. Both galleries are uncorrected for extinction.

The May 31 (O5JV01) observation occurred during the completely opaque phase of the “iron curtain”. From this stage, based on our previous experience with V1974 Cyg and related ONeMg novae, we attempted to predict exposure times on the basis of the rate of development. The expansion velocity inferred from the width of the 1700Å pseudo-emission feature was approximately 4000 km s⁻¹ and, based on the the optical light curve, this nova appeared to be developing about 30% faster. Subsequent observations confirmed this behavior: it was always possible to find an identical phase for each spectrum to that of V1974 Cyg by scaling the time after optical maximum. From this point alone it is clear that the ejecta of the two novae were similar in dynamics and mass distribution that scaled with the energy of the outburst.

The second set of observations, June 22 (O5JV02), displayed strong P Cygni absorption troughs on many of the usually occurring strong resonance line profiles, as shown in Fig. 7. This stage is characteristic of ONeMg novae but not for classical novae of the CO type. We should add that two recurrent novae, U Sco during the 1979 outburst, and LMC 1990 # 2, also displayed strong P Cyg profiles on ultraviolet resonance lines of Si IV and C IV in IUE spectra. We will return to this point below in our discussion of Nova LMC 2000. The strongest absorption was found for Si IV 1400Å, which displayed a terminal velocity of -5200 km s⁻¹. This radial velocity is substantially larger than any obtained from the optical line profiles reported by Della Valle et al. (2002) for which the velocities are in closer agreement with those measured on emission lines observed during the August 29 observations (see below, sect. 3.2). In particular, H α on 31 May showed a weak P

²Accessible through URL: http://physics.nist.gov/cgi-bin/AtData/main_asd.

Cyg absorption at -2500 km s^{-1} , and low intensity red wing emission extending to -4000 km s^{-1} . This weak absorption had disappeared by 25 June, as had the extended wings on both sides of the line, being replaced by a nearly symmetric profile with FWZI of 4000 km s^{-1} . The Al II 2669Å and N IV 1486Å lines at this later epoch, obtained from our STIS spectrum, showed a nearly identical profile. There was still, however, significant overlying line absorption that likely altered some of the emission line characteristics. In particular, the He II 1640Å emission is flanked by numerous low ionization absorption features and also the wing of the emerging O III] 1667Å line. The Mg II profile shows a weak absorption feature at this stage extending about -4000 km s^{-1} with a deepest absorption at about -2500 km s^{-1} . The Mg II profile at the “matching epoch” of V1974 Cyg (see below), the spectrum LWP22786 (see Shore et al. 1993), displays a trough with deepest absorption at about -3000 km s^{-1} . None of the STIS spectra were taken early enough to reveal the strong P Cyg phase of this resonance doublet.

The P Cyg profiles also provide a clue to the origin of the photometric and spectroscopic scaling between V382 Vel and V1974 Cyg. The ratio of the maximum expansion velocity, derived from the P Cyg profiles was about 1.3 at the same epoch. It appears the luminosities of the central stars and the ejecta masses are about the same and that the scaling results from simply from the relative rate of decrease of the ejecta column density. The strength of the P Cyg absorption trough and the saturation of the profile, especially for the Si IV 1400Å lines, argues for a large covering fraction at this stage of expansion for the optically thick material. As we will describe below, the later (nebular) stages display line profiles are more consistent with an axisymmetric than spherical geometry for the ejecta. Therefore, as we found with V1974 Cyg and other ONeMg novae, the early optically thick stages reveal a different ejecta geometry than the slower moving material observed during the nebular stage.

The last observation with STIS occurred on August 29. By this time, the nova was in the nebular stage. Strong emission dominated the 1200-2000Å region, especially the resonance lines. Notably, [Ne IV] 1602Å was approximately half the intensity of He II 1640Å and displayed a nearly identical profile, but [Ne V] 1575Å was not observed. High ionization species included N V 1240Å, Si IV + O IV 1400Å and C IV 1550Å, but there is no trace of O V 1375Å. The N IV 1486Å line was strong but there is no visible emission at N IV] 1718Å. Resonance intercombination lines were strong, O III] 1667Å and Si III] 1895Å and C III] 1909Å being examples. Several comparatively low ionization species were still present, including O I 1300Å, C II 1335Å, N II 2145Å, and Mg II 2800Å. The FWHM for all these lines was about 4000 km s^{-1} , and the profiles were nearly identical (see discussion below).

3.2. Energetics and Reddening

Using $t_2 = 6$ days and $t_3 = 10$ days, Della Valle et al. (2002) derive $M_V(\text{max}) = -8.7 \pm 0.2(1\sigma)$ mag, which translates to $L_{\text{max}} \approx 2 \times 10^5 L_{\odot}$, and a distance of about 2 kpc. The first STIS observation occurred within one week of maximum visual brightness, at a time corresponding

approximately to t_2 . The second and third STIS observations were obtained long after visual maximum, by which time the flux maximum had clearly shifted into the ultraviolet. They permit an independent determination of the energetics of the outburst.

The spectrum obtained on May 21 most closely resembles the IUE spectrum SWP44156 of V1974 Cyg 1974 at about 20 days after optical maximum, the uncorrected ratio being a factor of 5 (Fig. 8) virtually independent of wavelength. The close correspondence of the spectra and the nearly independent flux ratio suggests the reddening for the two novae is similar and we will subsequently adopt $E(B-V)=0.2$ for V382 Vel in the analysis to follow.³ Only Mg II 2800Å was observed in emission during the first STIS spectrum. Its velocity width is consistent with that observed at H α . For a constant (positive) velocity gradient, the Mg II velocity indicates the line profile was formed from slower moving gas situated deeper in the ejecta than the region from which the resonance absorption trough, on the later-observed P Cyg lines, form. In support of this interpretation, we note that in the May 21 spectrum, we detect a weak P Cyg absorption feature at about -3000 km s^{-1} , consistent with the reported blueward Balmer line absorption velocities from the ESO spectra Della Valle et al. (2002).

For the June 21 observation, the integrated flux was $6.98 \times 10^{-8} \text{ erg cm}^{-2}\text{s}^{-1}$ from 1170 - 3070Å, uncorrected for extinction. The comparison is shown in Fig. 9 with V1974 Cyg (SWP 44378, taken about 50 days past optical maximum). Again, the flux ratio between the spectra is a factor of 5 in the region shortward of 1700Å, uncorrected for extinction. For August 29, the flux in this spectral range was $1.05 \times 10^{-8} \text{ erg cm}^{-2}\text{s}^{-1}$. At this stage, an approximate match is provided to V1974 Cyg with spectrum SWP 44378 taken 196 days after optical maximum. There are, however, significant differences that are clearly not the result of extinction. V382 Vel continued to display a strong O I $\lambda 1302$ emission even into the nebular phase and C IV $\lambda 1550$ was also stronger relative to the nitrogen lines. Al III $\lambda 1860$ remained stronger, and while the Si III]/C III] ratio is about the same as V1974 Cyg, the lines display considerably more knotted structure. This may be due, in part, to the resolution of the IUE low dispersion data but that cannot explain all the differences (see Fig. 9).

The interstellar Ly α profile provides additional information on the possible reddening, yielding a neutral hydrogen column density of $N_H \approx 1.2 \times 10^{21} \text{ cm}^{-2}$. For the August 29 spectrum, displayed in Fig. 10a, we assumed a Gaussian profile for the ejecta emission with a FWHM of $\approx 1500 \text{ km s}^{-1}$, scaled to the blue wing of the observed emission. At this epoch, there should have been no P Cyg absorption trough. The red wing of Ly α is blended with the N V profile producing the obvious discrepancy but we cannot obtain an unblended, unabsorbed N V profile with which to precisely model the interstellar absorption. Therefore, we concentrate on the blue wing of Ly α . It is clear

³We note that the Austin et al. (1996) value of $E(B-V)=0.3$ for V1974 Cyg is likely too large. A re-analysis of the spectrum is in preparation, but Draine & Tan (2002) find that adopting $E(B-V)=0.19$ for V1974 Cyg produces good agreement for a model of the X-ray scattering halo around this nova. In the present analysis, the *range* permitted for the reddening is 0.2 to 0.3.

the neutral hydrogen column density is high, this is supported by the strong H₂ absorption seen in the FUSE spectra (see discussion, below) and the strength of the interstellar lines (Table 5). Scaling E(B-V) = N_H/3.6 × 10²¹ cm⁻² (Savage & Mathis 1979) yields E(B-V) ≈ 0.3.

The first observations of V382 Vel (O5JV01) provide superb high quality interstellar line profiles from a wide range of absorbers. These include the CO (2-1) overtone transitions and, in the FUSE spectra, many H₂ lines. While a complete analysis of these data is beyond the scope of the present paper, a study is in preparation, we note here a kinematic constraint on the distance to this nova. An important feature of these spectra is that the Vela region is especially well observed in high resolution with both H I and ¹²CO (Burton 1985; Dame et al. 1987, 1999). The Galactic rotation curve determined by Brand & Blitz (1993) and standard stars observed in this direction yield a mean $v_{\text{LSR}} \approx -20 \text{ km s}^{-1}$. There is, however, a particularly interesting feature of the ¹²CO maps, a spur at large positive LSR velocity, +20 km s⁻¹, due to the Carina arm that is also present in the stronger interstellar lines in V382 Vel, requiring a lower limit on the distance of about 2 kpc. Sample profiles are displayed in Fig. 10b.

Assuming E(B-V)=0.2, the measured continuum fluxes for the three STIS observations are 3.67×10^{-7} (May 31), 3.02×10^{-7} (June 21), and $4.56 \times 10^{-8} \text{ erg s}^{-1} \text{ cm}^{-2}$ (August 29) from 1170–3100Å. At the time of the first observation, the optical flux, based on published UBV photometry, was $5 \times 10^{-8} \text{ erg s}^{-1} \text{ cm}^{-2}$. Even the first STIS observation shows that the UV corresponded to most of the emitted flux. This yields a total luminosity in the observed band of $> 4.9 \times 10^4 L_{\odot}$ for a distance of at least 2 kpc. If the distance is increased to 2.5 kpc, this luminosity becomes nearly identical with V1974 Cyg, about $8 \times 10^4 L_{\odot}$, about the Eddington luminosity of a 1.4 M_⊙ white dwarf (WD) (Shore et al. 1994). In their study, Della Valle et al. (2002) assumed virtually no reddening. For E(B-V)=0, we find integrated fluxes of 9.57×10^{-8} , 6.92×10^{-8} , and $1.05 \times 10^{-8} \text{ erg s}^{-1} \text{ cm}^{-2}$, in the respective STIS spectra, that are incompatible with the distance and spectral comparison with V1974 Cyg. The flux ratios between the short wavelength spectra of the two novae (see Fig. 9), assuming at least as great an extinction for V382 Vel as V1974 Cyg, gives a distance of 2 kpc assuming a 3.1 kpc distance for V1974 Cyg (see Paresce et al. 1995).

We can place independent constraints on the reddening using the quiescent luminosity. This comes from the pre-outburst observations using the parameters we have derived. Post-outburst GHRS spectra of V1974 Cyg revealed a white dwarf with $T_{\text{eff}} \approx 2 \times 10^4 \text{ K}$ after 3 years. While we do not know if an accretion disk was established by that time, it is likely one was present for V382 Vel before outburst. Taking $V = 16.6$ and assuming a distance of 2 kpc, the visible colors alone give $L \approx 0.3 L_{\odot}$. For an accretion disk with a $\nu^{1/3}$ spectral energy distribution, this becomes $L > 2 L_{\odot}$ longward of 1200Å. The luminosity is not unusual for novae entering the later stages of outburst, and is higher than the last GHRS spectrum we obtained for V1974 Cyg.

We summarize our distance determinations as follows. From the maximum magnitude - rate of decline (MMRD) relation, Della Valle et al. (2002) obtain a distance of 2 kpc. Based on comparisons with V1974 Cyg and Nova LMC 2000 (see below), we obtain the range 2 to 3 kpc. Interstellar lines

constrain the nova to be at least at the distance of the Carina arm, so > 2 kpc. The preoutburst luminosity yields 2 kpc while $L_{\max} \leq L_{\text{Edd}}$ gives 2.5 kpc for a Chandrasekhar mass white dwarf.

3.3. Line Profiles

The first emission lines to appear were the strongest permitted and intercombination transitions, O I 1302Å, N II] 2145Å, Al II 2675Å, and Mg II 2800Å. These showed identical profiles to the optical transitions. As described by Hayward et al. (1996) and Shore & Starrfield (1998) for V1974 Cyg, the optical lines suffer less absorption within the ejecta and deeper layers are observed first at longer wavelengths. The consistency of the structure over time indicates that the observed emission knots must have formed early in the outburst – most likely at the time of ejection.

Balmer line profiles obtained on 25 June show strongly asymmetric structure, with a well defined peak at $+800 \text{ km s}^{-1}$ and an uncorrected $\text{H}\alpha/\text{H}\beta$ ratio of about 6.8 Della Valle et al. (2002). Assuming case A recombination for the highest velocity – and presumably most transparent – portions of the line profile, this corresponds to $E(\text{B-V}) \approx 0.2$. This is consistent with our other determinations. Several distinct knots appear on all three principal Balmer profiles, at $+200$, $+400$ and $+800 \text{ km s}^{-1}$ with a weak extended feature at approximately rest (observer's frame). No corresponding knots are seen on the blueshifted side of the profile. Broad low intensity wings appear on all three profiles, the broadest is $\text{H}\delta$ extending to HWZI of 4000 km s^{-1} while the other two lines show only around 200 km s^{-1} (Fig. 11).

A curious feature of the Balmer line profile development is the change in symmetry between the two epochs, separated by only about 30 days. The spectra in the first observation are almost identical to the low ionization inter-system lines observed in the June 21 spectrum. For instance, Al II $\lambda 2675$ with stronger emission on the blueshifted side of the profile, while the later spectra do not resemble any of the UV profiles. Later spectra are nearly symmetric. We note that a comparison of these low ionization profiles with the reported detection of Li I 6708Å (Della Valle et al. 2002) suggests that the latter is likely some other low ionization emission centered at around 6705Å. Given the nitrogen enhancement seen in this nova, a likely candidate is the doublet N I (${}^4\text{P}^o - {}^4\text{D}$) 6704.84, 6706.11Å.

The far ultraviolet emission spectrum was sparse. We show in Fig. 12 the region of $\text{Ly}\beta$ and the O VI 1031, 1036Å doublet. These were the only strong emission lines detected in the FUSE spectra, taken within 1.5 years of outburst. The O VI doublet had a profile that was very similar to the optically thin C IV 1550Å doublet which, as we found for V1974 Cyg, is consistent with the combined optically thin profiles of the doublet components whose intrinsic form is similar to the singlets seen in the STIS spectra (this is also seen in the STIS profile of the O III] 1667Å multiplet). The O VI doublet showed strong decrease between the 2000 February and 2000 July spectra, dropping from $9.3 \times 10^{-12} \text{ erg s}^{-1}\text{cm}^{-2}$ to $2.0 \times 10^{-12} \text{ erg s}^{-1}\text{cm}^{-2}$ (A09303/4). Both these fluxes are uncorrected for extinction but have been corrected for line absorption. The FWHM

remained about 1000 km s^{-1} . The observed decline is completely consistent with the expected t^{-3} power law for the emission (a factor of about 3.9) from a freely expanding shell. No Lyman series emission lines were seen in either FUSE observation; recall that Ly α showed a strong P Cyg profile in 1999 June but this emission was absent in the 1999 August observation.

The line profiles are virtually identical for all components of even the blended multiplets by the third STIS observation, adding weight to the assertion that the ejecta were optically thin (nebular) by this stage. We compare the profiles of He II $\lambda 1640$ and [Ne IV] $\lambda 1602$ in Fig. 13. Notice that the near identity of the profiles also argues for chemical homogenization of the ejecta during the explosion. There are no indications of the deviations we found for V1974 Cyg among the individual knots and these knots in the UV line profiles can also be identified between wavelength regions and at different epochs. We remark, however, that these are *not* spatially resolved and the integrated large aperture spectra for V1974 Cyg also did not reveal large deviations. For example, the Balmer emission lines were more asymmetric in V382 Vel within the first 3 weeks after outburst than the UV lines observed later with STIS. They quickly transformed, however, to the same emission structure (by June 2) that was observed almost 3 months later in the UV and on other optical lines. The knot at $+850 \text{ km s}^{-1}$ is particularly strong in both the Balmer and UV lines until 25 June. This is not unexpected, since the ejecta expand hypersonically and individual knots had not yet recombined by the third STIS observation. The later STIS profiles are more symmetric than those seen in the first observations in the optical and with STIS.

In an attempt to determine more information about the structure we performed a Monte Carlo simulation as described in Shore et al. (1993). Two geometries were assumed: a spherical shell, and a thin ring. For each, a linear velocity law was assumed and the profile was rebinned in the observer’s frame. The maximum velocity was fixed at 5200 km s^{-1} using the P Cyg profiles on the UV resonance lines whose terminal velocities *always* exceeded those of the optical Balmer lines and the later emission line profiles. Figure 14 shows the comparison of a sample model profile with N IV] 1486\AA and He II $\lambda 1640$. Both are assumed to be an optically thin recombination transitions. The model profile can also be compared with other lines in Fig. 6. The line is mainly formed from comparatively low velocity gas so we explored a range of maximum velocities for the model. The good agreement was found for a spherical geometry with $\Delta R/R = 0.7$ and the density varied as $n(R) \sim R^{-3}$ for a constant shell mass. For a ring, almost the same profile is obtained for $\Delta R/R = 0.5$ for an inclination of 25° . There is a near degeneracy between the inclination and thickness for a ring, but the relative weakness of the extended wings on the ring profile suggest that the spherical case more closely matches the data. However, we venture the suggestion that V382 Vel may, when spatially resolved, contain an elliptical ring with a transverse expansion rate of $0.2 \text{ arcsec yr}^{-1}$ for a distance of 2.3 kpc. Our model is derived *for this optically thin stage*. There must be additional, rapidly expanding matter – as we found for V1974 Cyg – in a more spherical distribution to account for the broad shallow wings observed on all emission line profiles in the earlier spectra.

A range of inclinations can be estimated using the observed outburst amplitude and the range

in the determined distance. The absolute quiescent magnitude, uncorrected for inclination, for very fast novae is 3.76. At distances between 2 and 3 kpc, the inclination range required to produce the observed, apparent quiescent magnitude lies between 45 and 67 degrees assuming an $E(B-V) = 0.25$. This differs from the value obtained by line profile analysis so imaging the spatially resolved ejecta should decide this issue.

As seen from Fig. 14, the fit seems to be quite good but since the models “knots” are randomly generated, this comparison suggests that there is nothing particularly informative in the distribution of the knots, that they are not related directly to the large scale structure of the ejecta. Rather, we are likely seeing the frozen remnants of an instability that produced them early in the outburst. A wind-like velocity law, $v \sim (1 - R_\star/r)^\beta$, where R_\star is the stellar radius and β is a constant, fails to reproduce the line profile, supporting the contention that the ejecta are freely expanding and not a wind, at least at the later stages. This does not rule out possible wind-ejecta interactions as a source for hard X-ray emission observed early in the outburst (Mukai & Ishida 2001, Orio et al. 2001). The bulk of the line emission comes from the innermost portion of the ejecta. This is also true for the optical line profiles, which in general sample the denser parts of the ejecta at an earlier time than the UV (see e.g. Hayward et al. 1996). While a detailed model is beyond the scope of this paper, we note that the resemblance of the UV lines in the third STIS spectrum with the first optical data suggests they are formed in the same part of the ejecta and could be used for detailed modeling.

It is interesting also to note the weak dependence of profile on ionization state. The Ne IV] 1602Å line may have a contribution from a more spherical distribution (see Shore et al. (1993) for discussion), although the peaks in the line core are indicative of a mainly an axisymmetric geometry, while He II 1640Å and N IV] 1486Å wings are narrower and likely formed in a predominantly ring-like structure. Any further discussion of these kinematic profiles would, however, be overinterpretation. It suffices that the basic shell appears to be comparatively thick and extended and, as we will show in the next section, agrees with the results of detailed photoionization models.

The third STIS spectrum provides the strongest evidence for homogeneity of the ejecta. The Ne IV] 1602Å and He II 1640Å lines show identical profiles, with matches for each knot. This contrasts with our GHRS results for V1974 Cyg ? where high spatial resolution small aperture spectra show marked contrasts between these two lines and also with C IV 1550Å. Closer agreement was found for that nova between line profiles earlier in the outburst at a time similar to those reported here, suggesting that we were not yet completely viewing the ejecta.

4. Photoionization Model Analysis

The *CLOUDY* 94.00 photoionization code (Ferland et al. 1998, and references therein) was used to model the observed emission line fluxes for the August 29 observation given in Table 2. We concentrate on this set of spectra since by this stage the ejecta were sufficiently optically

thin, as indicated by the near identity of the line profiles on all species. *CLOUDY* simultaneously solves the equations of thermal and statistical equilibrium for a model emission nebula. Its output, the predicted flux of $\sim 10^4$ emission lines, is compared against the observations to determine the physical conditions in the shell. *CLOUDY* has been used to model numerous novae (see Schwarz et al. 1997, 2001; Vanlandingham et al. 1996, 1997, 1999).

The outer radius of the model shell is constructed using the observed maximum expansion velocity and the time since outburst. From the early P Cygni terminal velocities, we use 5200 km s⁻¹ and assume a linear velocity flow to set the outer dimension of the shell. The inner radius was determined from the estimated shell thickness of 0.5. The ejecta are assumed to be spherically symmetric. The density of the shell is set by a hydrogen density parameter which has a power law density profile with an exponent of -3. This provides a constant mass per unit volume throughout the model shell, which is a reasonable assumption. *CLOUDY* also allows a filling factor of less than one. The filling factor sets the ratio of the filled to vacuum volumes in the ejecta. It acts by modifying the volume emissivity and the optical depth scale of the ejecta. The elemental abundances are set relative to hydrogen and we began initially with V1974 Cyg abundance solution (Vanlandingham et al. in prep). A hot (few 10⁶ K) non-LTE planetary nebula nuclei spectral energy distribution (Rauch 1997) with a high luminosity ($\sim 10^{38}$ erg s⁻¹) is used as the input source.

Initial attempts to reproduce the observed line flux did a reasonable job fitting the majority of the lines but failed with the highest ionized species. The high density and the low luminosity of the model produced an ionization bounded shell with a hydrogen recombination radius slightly larger than the inner radius. As a result, the high ionization zones in the model shell were small and did not produce the required amount of flux. In order to include these other lines we added an additional, less dense component to the previous model. The lower density means the ionizing photons penetrate further into the model shell, resulting in a hotter and more ionized shell. The second component has exactly the same parameters as the denser component except for the hydrogen density and filling factor which was allowed to vary independently. Table 3 gives the comparison between the observations and the *CLOUDY* predictions for the two models. Three of the lines from Table 2 may be blends based on the *CLOUDY* predicted fluxes from lines of similar wavelengths. These lines are noted as “Blend” in Table 3 and all of the *CLOUDY* lines within a few Angstroms are summed and their combined flux is compared with the observation. The fluxes are presented relative to the He II (1640Å) line since we lack any uncontaminated hydrogen lines in the spectrum. The observed lines were dereddened with $E(B - V) = 0.2$. We determined a goodness of fit from the χ^2 of the model:

$$\chi^2 = \sum_i \frac{(M_i - O_i)^2}{(\sigma_i)^2}, \quad (1)$$

where O_i is the observed line ratio and σ_i is the error associated with the observed line ratio (\sim

25%). The total χ^2 of the combined models is ~ 17 with the largest contribution coming from the N V line which is blended with the Ly α . The best fit model parameters are given in Table 4. There are 13 free parameters in the two *CLOUDY* models and thus with 16 line ratios to model there are 3 degrees of freedom. The metal abundances are scaled to He so if He/H>1, the metallicity is automatically elevated. The derived ejected mass of the models is on the high end of the values typically found for novae, $M_{\text{ejecta}} \sim 5 \times 10^{-4} M_{\odot}$, assuming a spherical covering factor of one. The covering factor is the fraction of 4π str covered by the model shell and it scales with the *CLOUDY* line luminosities. Note, a covering factor less than unity doesn't affect the model WD luminosity since the covering factor only scales the line luminosities associated with the model shell.

The derived abundances are not as extreme for V382 Vel as those we have determined for “fast” novae, especially the Galactic novae V693 CrA and V838 Her, and Nova LMC 1990# 1. Helium, carbon, and silicon are consistent with solar abundances (He = 1.0, C = 0.6 ± 0.3 , Si = 0.5 ± 0.3), while nitrogen, oxygen, neon, magnesium, and aluminum are enhanced (N = 17 ± 4 , O = 3.4 ± 0.3 , Ne = 17 ± 3 , Mg = 2.6 ± 0.1 , Al = 21 ± 2). In general, the nitrogen, neon, and aluminum enhancements are lower than either V693 CrA or Nova LMC 1990 # 1. A more detailed comparison with other ONeMg novae, including a re-analysis of V1974 Cyg data, will be presented in a future paper.

An independent estimate of the distance can be obtained using the the observed He II flux and the predicted He II luminosity from the combined models. The observed flux was dereddened assuming an $E(B - V) = 0.2$ and the model luminosities were calculated with a covering factor of unity. The distance obtained using this method, $2.8 C^{1/2}$ kpc where C is the model covering factor, is in agreement with our previous determination of ~ 2.5 kpc. If we use 2.5 kpc as the true distance the covering factor of the combined models must be 0.8 which drives the ejected mass down to $4 \times 10^{-4} M_{\odot}$. The mass derived by Della Valle et al. (2002) is $6.5 \times 10^{-6} M_{\odot}$ from the data on 2000 Oct. 2 for an assumed distance of 1.7 kpc. Increasing this to 2.3 kpc increases the estimated mass to $2 \times 10^{-5} M_{\odot}$, still nearly a factor of 10 below the one we derive based on the UV spectra. However, since this nova suffered an extended “iron curtain” phase in the UV, the minimum mass must have been significantly higher than that estimated by Della Valle et al. (see Shore 2002).

5. Comparisons with Nova LMC 2000

Nova LMC 2000 provides a comparison with V382 Vel, even more so than V1974 Cyg. It too was an ONeMg nova, but being situated in the LMC provides absolute information on distance against which the Galactic novae can be scaled. Having observed this nova in two nearly identical stages to those seen in V382 Vel, we here make some brief remarks about what can be learned from the comparative developments (a more detailed paper on Nova LMC 2000 is in preparation).

Nova LMC 2000 was discovered by Liller on 2000 July 12.4 UT (Liller & Stublings 2000).

Archival images (Duerbeck & Pompei 2000) show the outburst was not detected on June 29.38 but the nova was visible a very short time later, June 29.65. Its maximum measured visual magnitude was 11.2. Optical spectra taken within two days showed emission lines of neutral and singly ionized species, especially the Na I D lines, and P Cygni profiles with a maximum expansion velocity of -1900 km s^{-1} (Duerbeck & Pompei 2000).

Our STIS observations employed the same settings as those we used for V382 Vel and occurred on 2000 August 19.7 UT and August 20.9 UT (Shore et al. 2000). Weak iron-peak absorption may still be present, especially from 1550 to 1565Å. The spectrum strongly resembled the August 29 V382 Vel spectrum but with much stronger Ly α and Si III] 1895Å and C III] 1910Å emission, with Si III]/C III] about 2. Strong C IV P-Cyg absorption was seen with a terminal velocity of 2000 km s $^{-1}$, similar to the FWHM velocity for the emission lines. The strongest emission lines were C III 1076Å, N V 1240Å, N III/O III 1267Å, O I 1304Å, C II 1334Å, Si IV/O IV] 1400Å, C IV 1550Å, He II 1640Å, O III] 1667Å, N III] 1750Å, Si II 1816Å, Al III 1860Å, Si III] 1895Å, C III] 1910Å, N II] 2145Å, C II 2321Å, Al II 2672Å, and Mg II 2800Å. Unlike V382 Vel at this stage, there were no N IV] 1486Å or 1718Å lines. The Ly α line remained strong and asymmetric. A comparison of the V382 Vel and Nova LMC 2000 Ly α profiles is shown in Fig. 15. Notice that the shift of the nova relative to the foreground Galactic contribution is responsible for the stronger blueshifted emission for the LMC nova and shows that the probable reason for the lack of recognition of Ly α P Cyg profiles in Galactic novae is due to interstellar absorption. This is displayed at higher resolution in the top panel of Fig. 15.

The first STIS spectrum was obtained at a later stage of the outburst than for V382 Vel. The metallic absorption lines had already largely disappeared, leaving strong P Cyg profiles on the UV resonance lines. It is important to note that this supports the conclusion drawn from Galactic systems that ONeMg novae systematically pass through this stage in the ultraviolet. The emission line profiles in the second STIS spectrum, even at this relatively early stage in the outburst, showed similar fine structure to those at the same stage in V382 Vel and V1974 Cyg. The integrated flux from 1150 to 3120Å was $8.6 \times 10^{-11} \text{ erg cm}^{-2} \text{ s}^{-1}$, which corresponds to $5.6 \times 10^{-10} \text{ erg cm}^{-2} \text{ s}^{-1}$ corrected for a field LMC reddening law with $E(B-V) = 0.2$. Adopting a distance of 52 kpc, this corresponds to $4.4 \times 10^4 L_\odot$ in the UV range *only*, since at this epoch most of the flux was being emitted in the ultraviolet. In view of the similarity of the spectra, these data yield a distance for V382 Vel of 3 kpc assuming its reddening is $E(B-V) = 0.2$, which is probably an upper limit for the distance of V382 Vel.

6. Summary and Conclusions

The analysis of V382 Vel along with two other ONeMg novae, V1974 Cyg and Nova LMC 2000, reveals a remarkable consistency in outburst characteristics among novae of this type. Although there is a range of masses and abundances, the energetics and spectral development closely follow each other. We derive a range for $E(B-V)$ of 0.2 to 0.3, with the most likely value being in the lower

end of the range based on a number of independent determinations, including the comparison with the other two well observed ONeMg novae. The maximum expansion velocity, of $> 5000 \text{ km s}^{-1}$, exceeds most novae of this class (except V838 Her (Vanlandingham et al. 1996) and LMC 1990 No. 1) and is consistent with the “fast” classification. The derived mass of $4 - 5 \times 10^{-4} M_{\odot}$ based on our analysis is at the upper end of the range determined for fast ONeMg novae. This mass estimate is, however, dependent on the ejecta filling factor which is difficult to precisely determine. Abundance enhancements relative to solar values are found for N, Ne, Mg, and Al, while He, C, and Si are approximately solar abundance. In general, the enhancements are lower than previously determined values for most ONeMg novae. Finally, although the system geometry is unknown, profile modeling suggests it is consistent with an inclined ring, with an angle of about 25° , that should be resolvable within a few years if the distance is about 2 to 3 kpc.

We warmly thank Howard Lanning, Tom Ake, B-G. Anderson, and George Sonneborn for their generous help with the STIS and FUSE observations. We thank Massimo Della Valle for communicating electronic versions of his ESO spectra in advance of publication and Karen Vanlandingham for insightful discussions. We also thank the referee for helpful remarks. The V382 Vel STIS spectra were obtained through an award of Director’s Discretionary Time and we thank Steve Beckwith for his support of these observations. Support for proposal GO 8540 and GO 8671 was provided by NASA through grants from Space Telescope Science Institute, which is operated by Associated Universities for Research in Astronomy, Inc., under NASA contract 5-26555. This work was supported by STScI under programs GO 8540 and GO 8671 and by NASA under the FUSE guest investigator program as project A093. SNS wishes to thank Profs. M. Salvati and F. Pacini for their kind hospitality during extended visits to Arcetri. SS, RDG, and CEW, and PHH acknowledge support of NSF and NASA grants to ASU, University of Minnesota, and University of Georgia, respectively.

REFERENCES

- Austin, S.J., Wagner, R. M., Starrfield, S., Shore, S. N., Sonneborn, G., & Bertram, R. 1996, AJ, 111, 869
- Brand, J. & Blitz, L. 1993, A&A, 275, 67
- Burton, W. B. 1985, A&AS, 62, 365
- Dame, T. M. et al. 1987, ApJ, 322, 706
- Dame, T. M. 1999, The Physics and Chemistry of the Interstellar Medium, Proceedings of the 3rd Cologne-Zermatt Symposium, held in Zermatt, September 22-25, 1998, Eds.: V. Ossenkopf, J. Stutzki, and G. Winnewisser, GCA-Verlag Herdecke, ISBN 3-928973-95-9, 100
- Della Valle, M., Pasquini, L., & Williams, R. 1999, IAU Circ., 7193, 1
- Della Valle, M., Pasquini, L., Daon, D., & Williams, R. E. 2002, A&A, 390, 155
- Draine, B. T., & Tan, J. C. 2002, *astro-ph/0208302*
- Duerbeck, H. W. & Pompei, E. 2000, IAU Circ., 7457, 1
- Ferland, G.J., Korista, K.T., Verner, D.A., Ferguson, J.W., Kingdon, J.B. & Verner, E.M. 1998, PASP, 110, 761
- Grevesse, N. & Noels, A., 1993, in Prantzos, de. N., Vangioni-Flam, E., & Casse, M., eds, Origin & Evolution of the Elements. Cambridge Univ. Press, Cambridge, p. 15
- Hayward, T. L. et al. 1996, ApJ, 469, 854
- Hidayat, B., Ikbal Arifyanto, M., Aria Utama, J., & Athiya, S. 1999, IAU Circ., 7188, 2
- Lee, S., Pearce, A., Gilmore, C., Pollard, K. R., McSaveney, J. A., Kilmartin, P. M., & Caldwell, P. 1999, IAU Circ., 7176, 1
- Liller, W. & Stubbings, R. 2000, IAU Circ., 7453, 1
- Morton, D. C. 1991, ApJS, 77, 119
- Mukai, K. & Ishida, M. 2001, ApJ, 551, 1024
- Orio, M. et al. 2001, MNRAS, 326, L13
- Payne-Gaposchkin, C. 1957, The Galactic Novae, New York, Dover
- Platais, I., Girard, T. M., Kozhurina-Platais, V., van Altena, W. F., Jain, R. K., & López, C. E. 2000, PASP, 112, 224

- Paresce, F., Livio, M., Hack, W., & Korista, K. 1995, A&A, 299, 823
- Rauch, T. 1997, A&A, 320, 237
- Schwarz, G.J., Starrfield, S., Shore, S.N., & Hauschildt, P.H. 1997, MNRAS, 290, 75
- Schwarz, G.J., Shore, S.N., Starrfield, S., Hauschildt, P.H., Della Valle, M., & Baron, E. 2001, MNRAS, 320, 103
- Shore, S.N., Sonneborn, G., Starrfield, S., Gonzalez-Riestra, R., & Ake, T.B. 1993, AJ, 106, 2408
- Shore, S.N., Sonneborn, G., Starrfield, S., Gonzalez-Riestra, R., & Polidan, R.S. 1994, AJ 421, 344
- Shore, S. N. 2002, International Conference on Classical Nova Explosions, Eds.: Hernanz J. and Josè, J. (NY: AIP Press), p. 175
- Shore, S. N. & Starrfield, S. 1998, Stellar Evolution, Stellar Explosions and Galactic Chemical Evolution, 413
- Shore, S. N. et al. 2000, IAU Circ., 7486, 1
- Steiner, J. E., Campos, R., & Cieslinski, D. 1999, IAU Circ., 7185, 2
- Vanlandingham K.M., Starrfield S., Wagner R.M., Shore S.N., & Sonneborn G. MNRAS, 1996, 282, 563
- Vanlandingham K.M., Starrfield S., & Shore S.N. 1997, MNRAS, 290, 87
- Vanlandingham K.M., Starrfield S., & Shore S.N. 1999, MNRAS, 308, 577
- Warner, B. 1987, MNRAS, 227, 23
- Woodward, C. E., Wooden, D. H., Pina, R. K., & Fisher, R. S. 1999, IAU Circ., 7220, 3

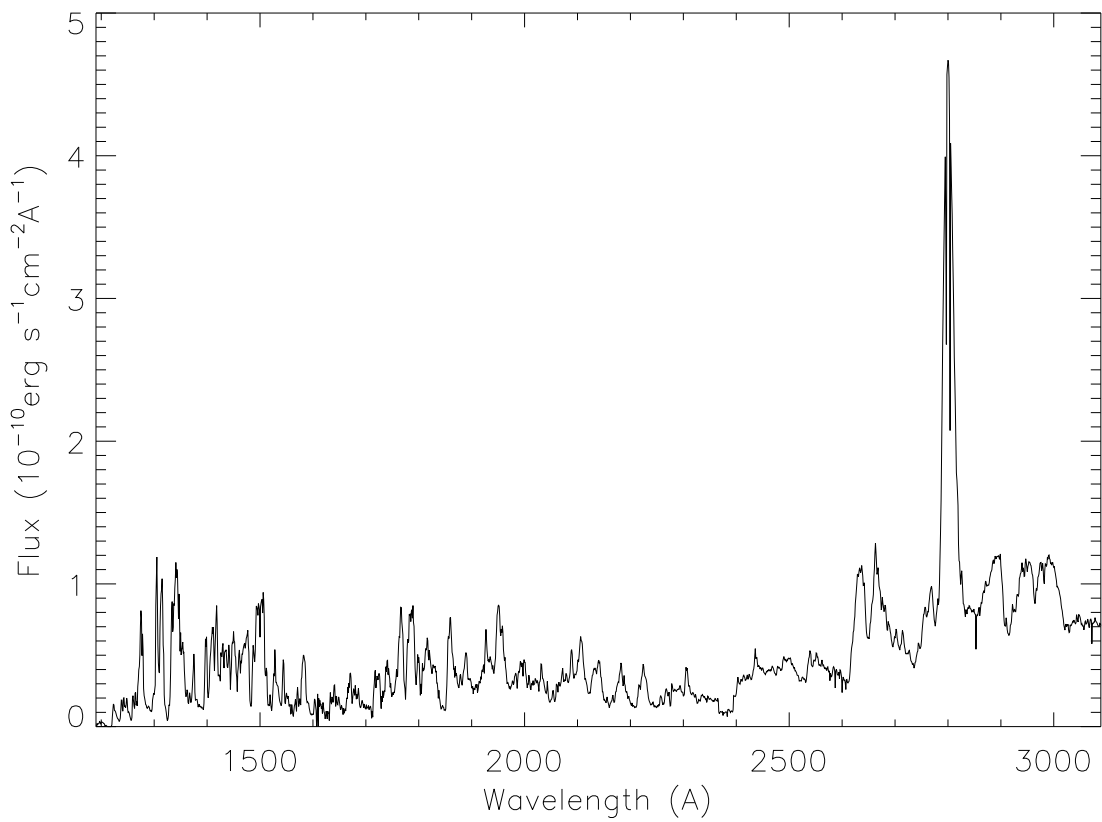


Fig. 1.— V382 Vel, 1999 May 31 (O5JV01) observation; absolute flux ($\text{erg s}^{-1}\text{cm}^{-2}\text{\AA}^{-1}$) with 1 \AA binning, uncorrected for reddening.

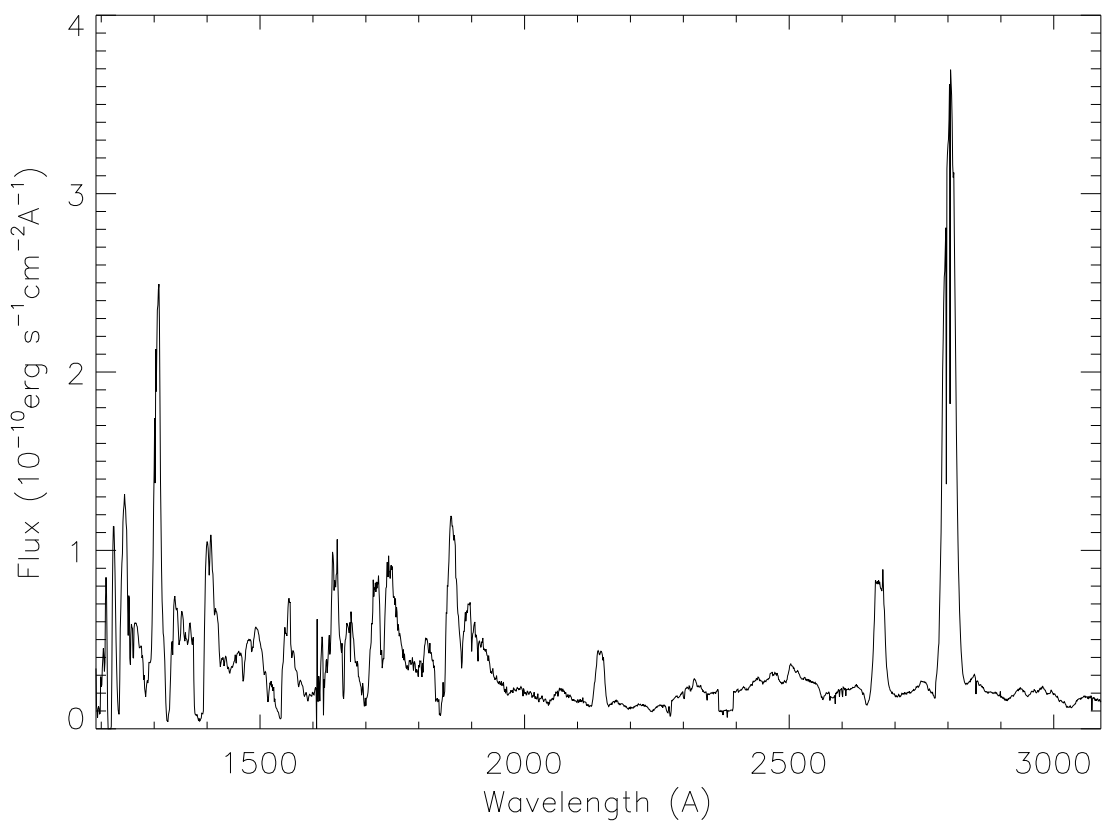


Fig. 2.— V382 Vel, 1999 Jun 21 (O5JV02) observation; same as Fig. 1

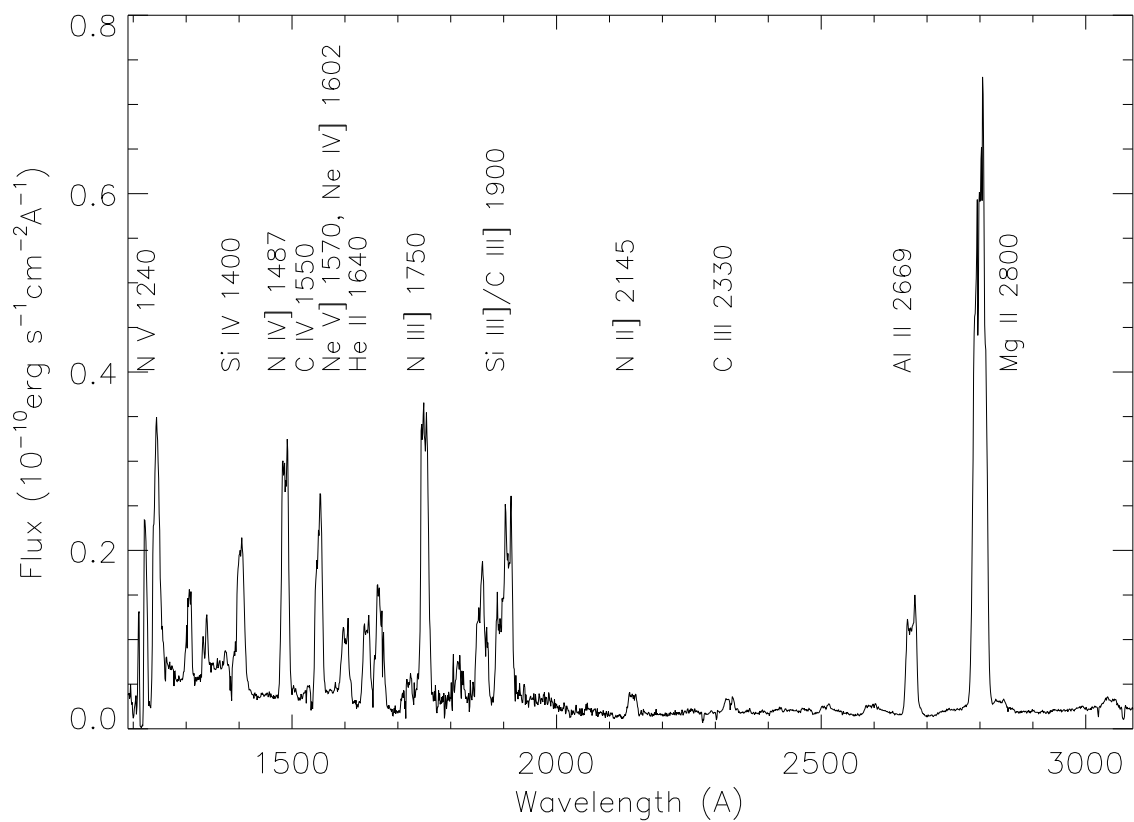


Fig. 3.— V382 Vel, 1999 August 29 (O5JV03) observation; same as Fig. 1

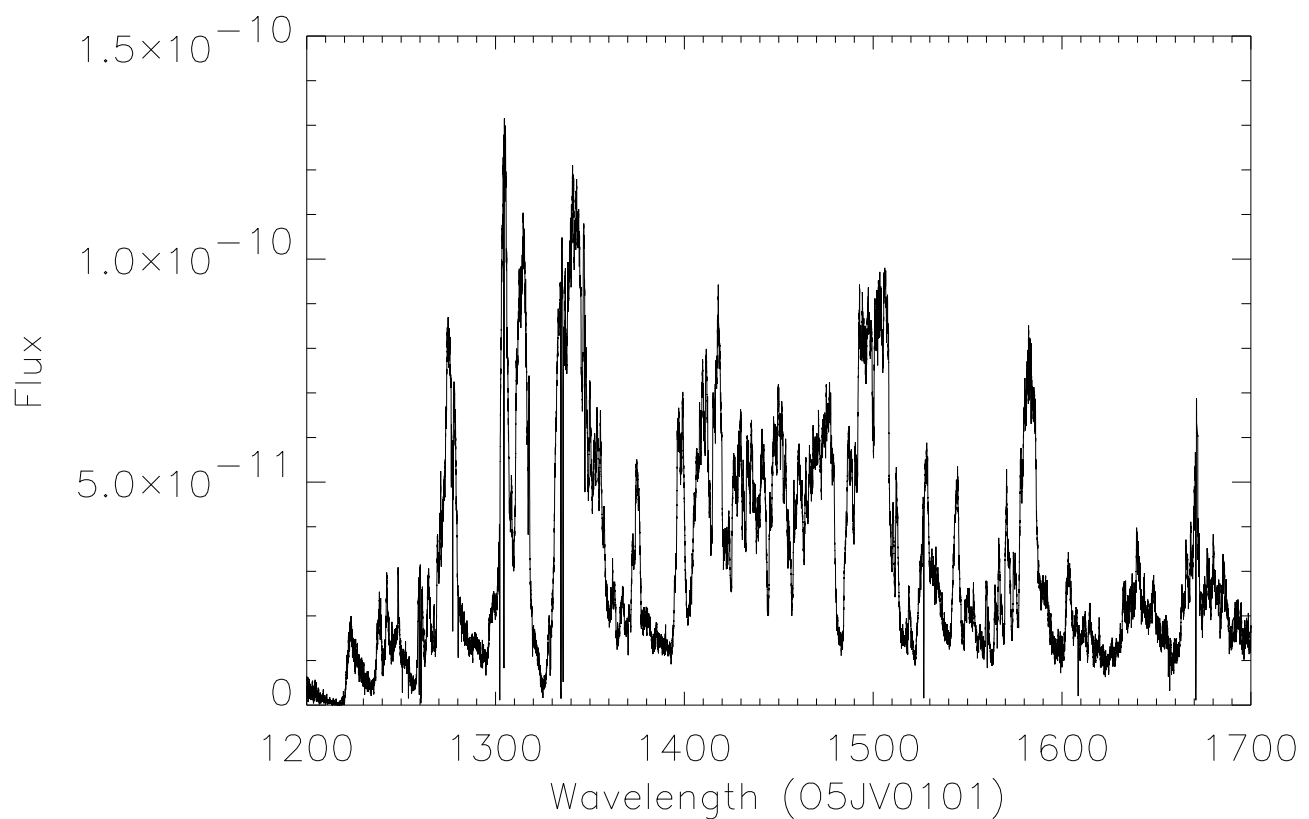


Fig. 4.— 1200 - 1700 Å region for 1999 May 31 (05JV01); same as Fig. 1

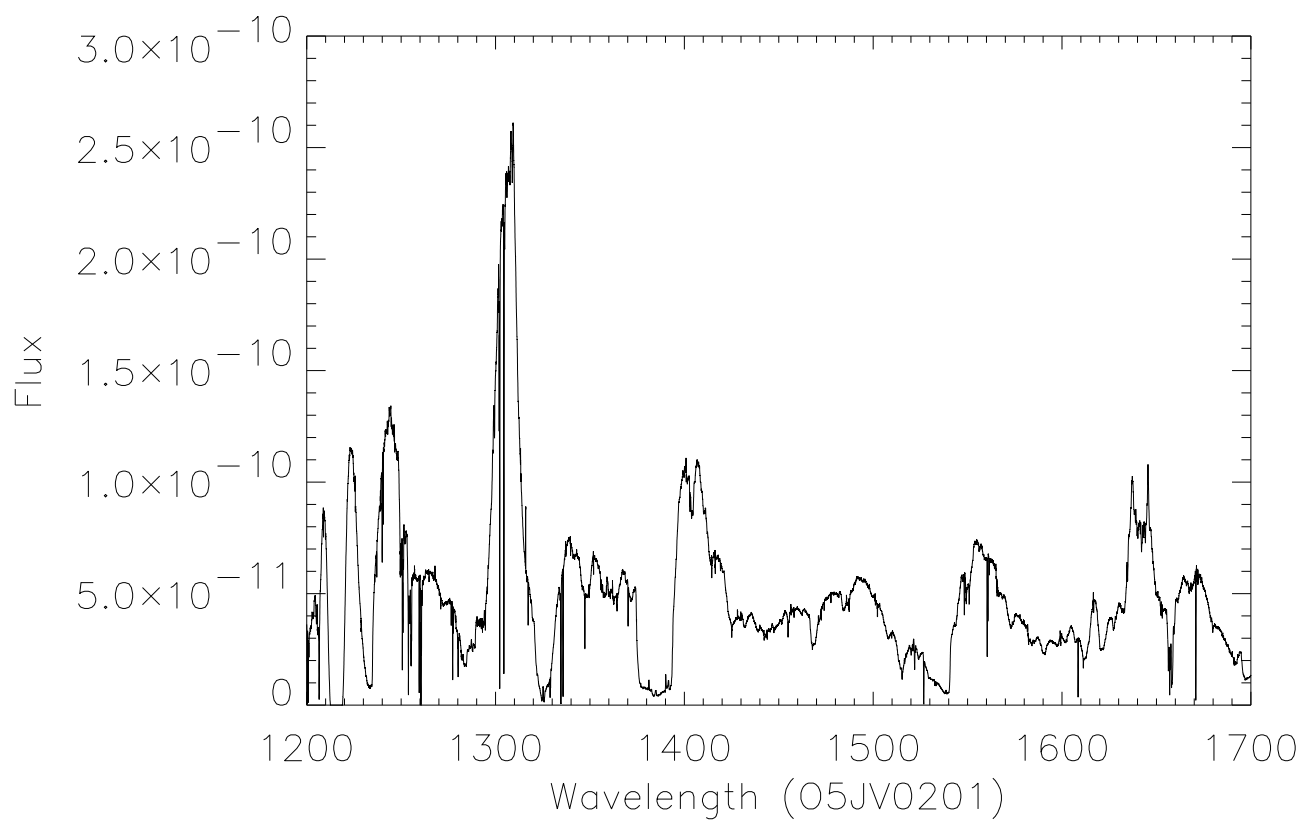


Fig. 5.— 1200 - 1700Å region for 1999 Jun 21 (O5JV02); same as Fig. 1

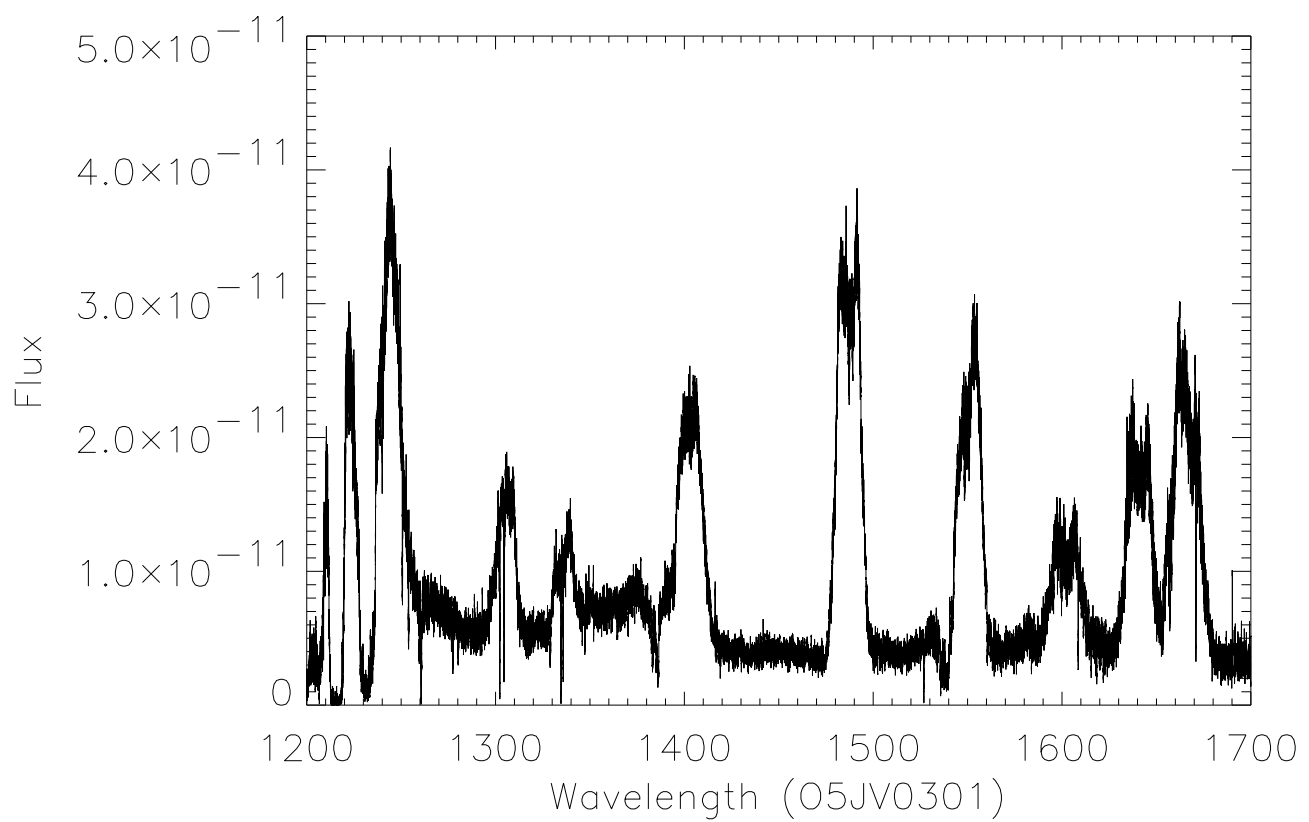


Fig. 6.— 1200 - 1700Å region for August 29 (O5JV03); same as Fig. 1

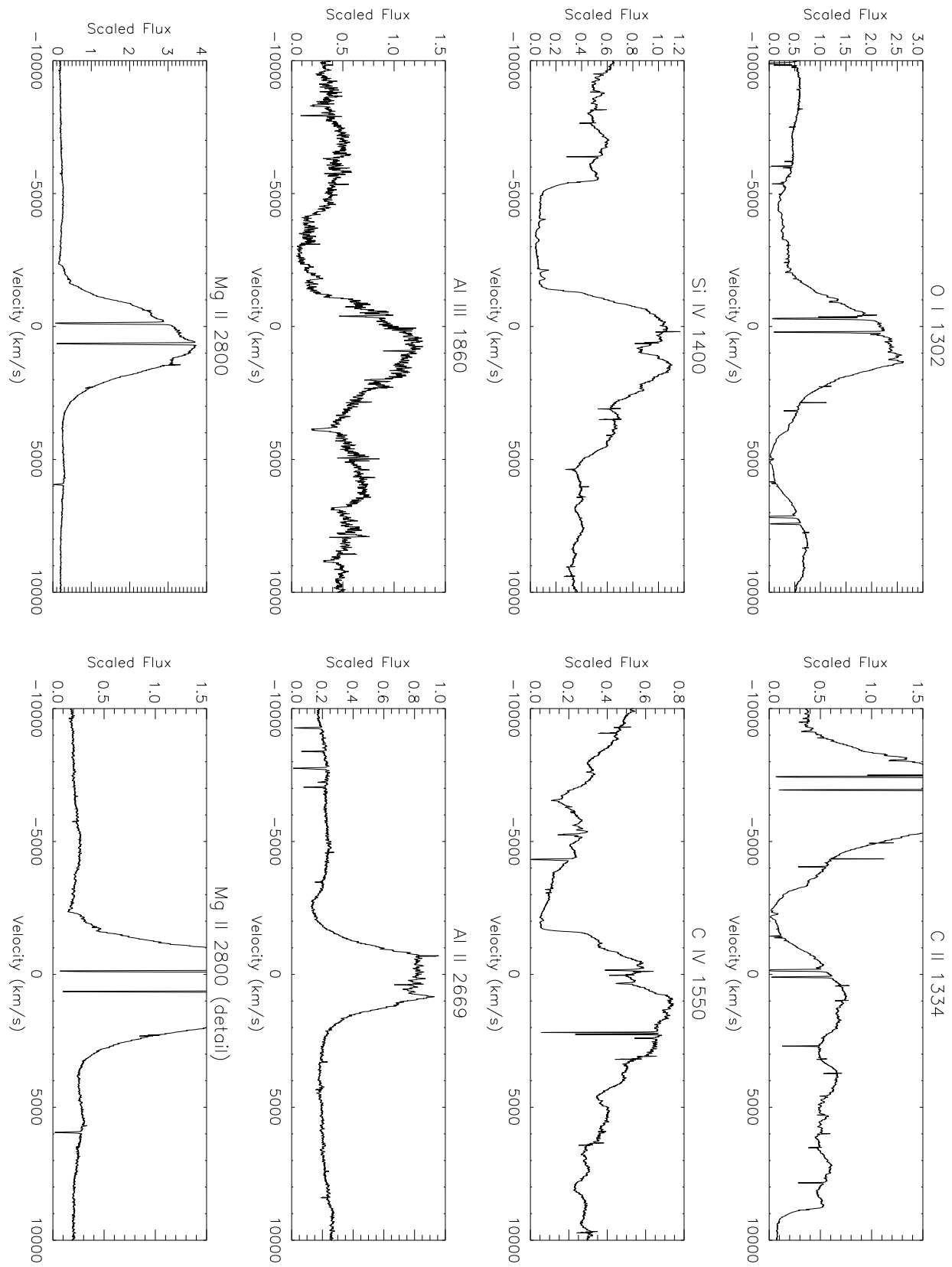


Fig. 7.— Resonance line profiles for the Jun 21 STIS spectrum of V382 Vel.

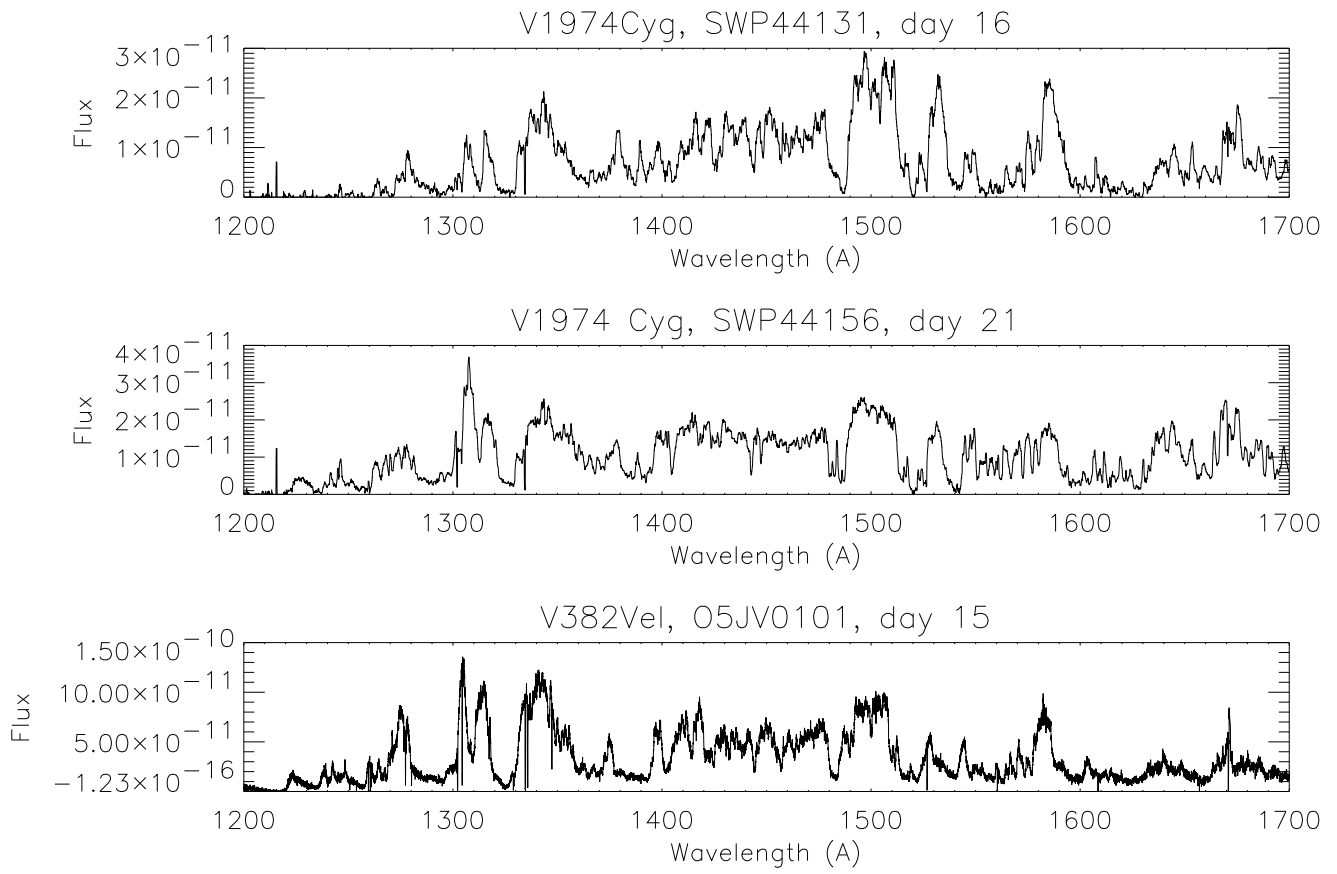


Fig. 8.— Comparison of two early high resolution spectra of V1974 Cyg with the 31 May observation of V382 Vel showing likely spectral development before the first STIS spectrum. No reddening corrections have been applied.

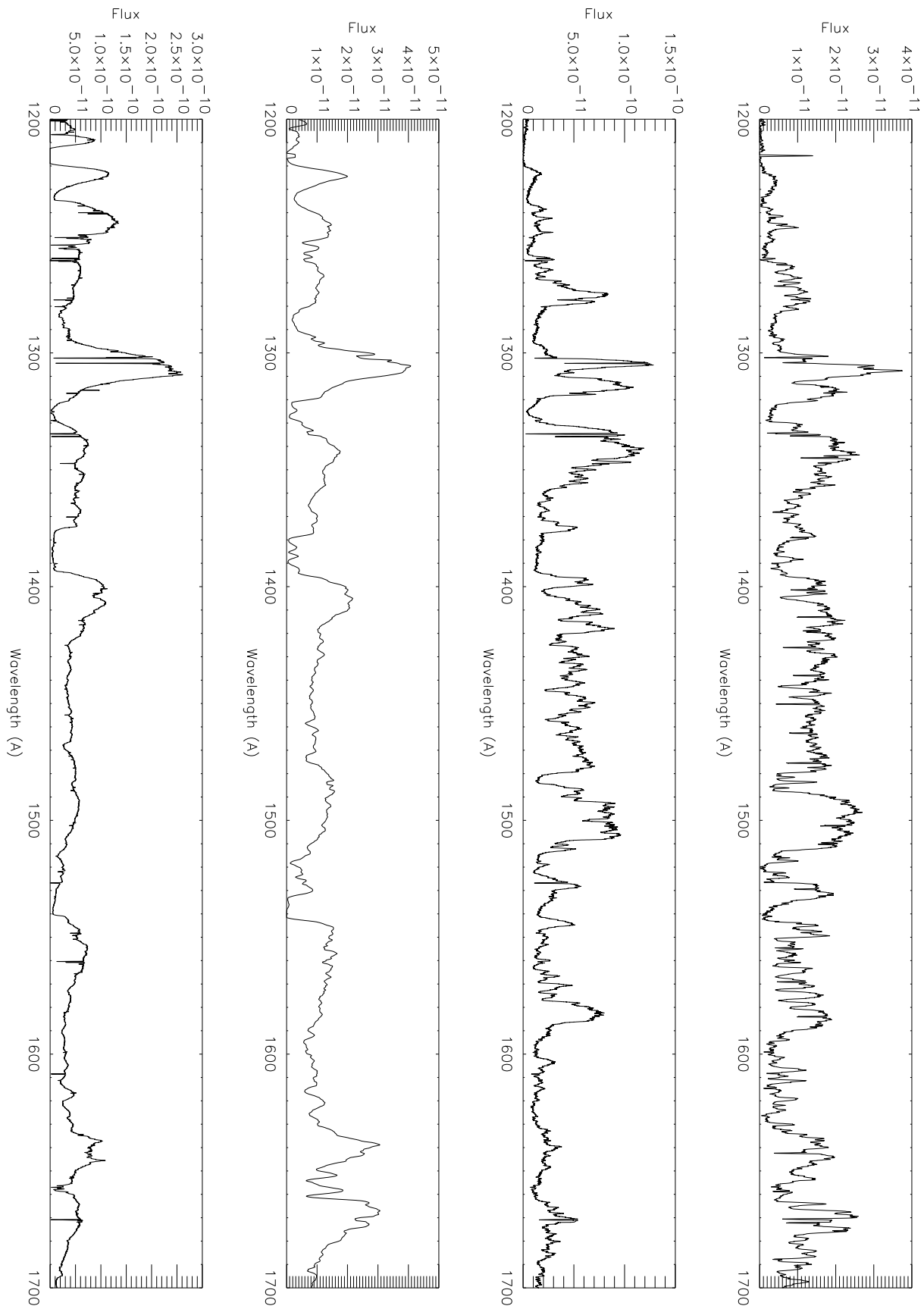


Fig. 9.— V1974 (top), SWP 44156; V382 Vel (second), O5JV01; V1974 Cyg (third), SWP 44378; V382 Vel (bottom), O5JV02. No reddening corrections have been applied.

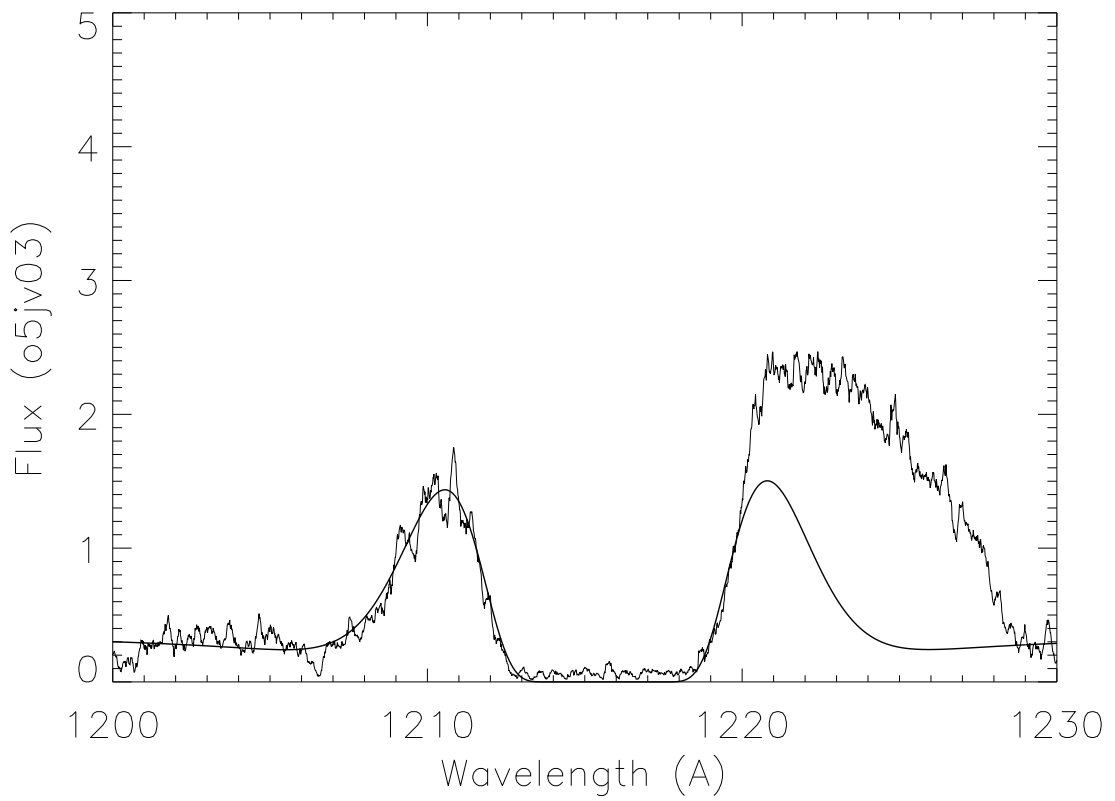


Fig. 10A.— A neutral hydrogen column density of $N_H \approx 1.2 \times 10^{21} \text{ cm}^{-2}$ model fit to the interstellar Ly α for the 1999 August 29 spectrum.

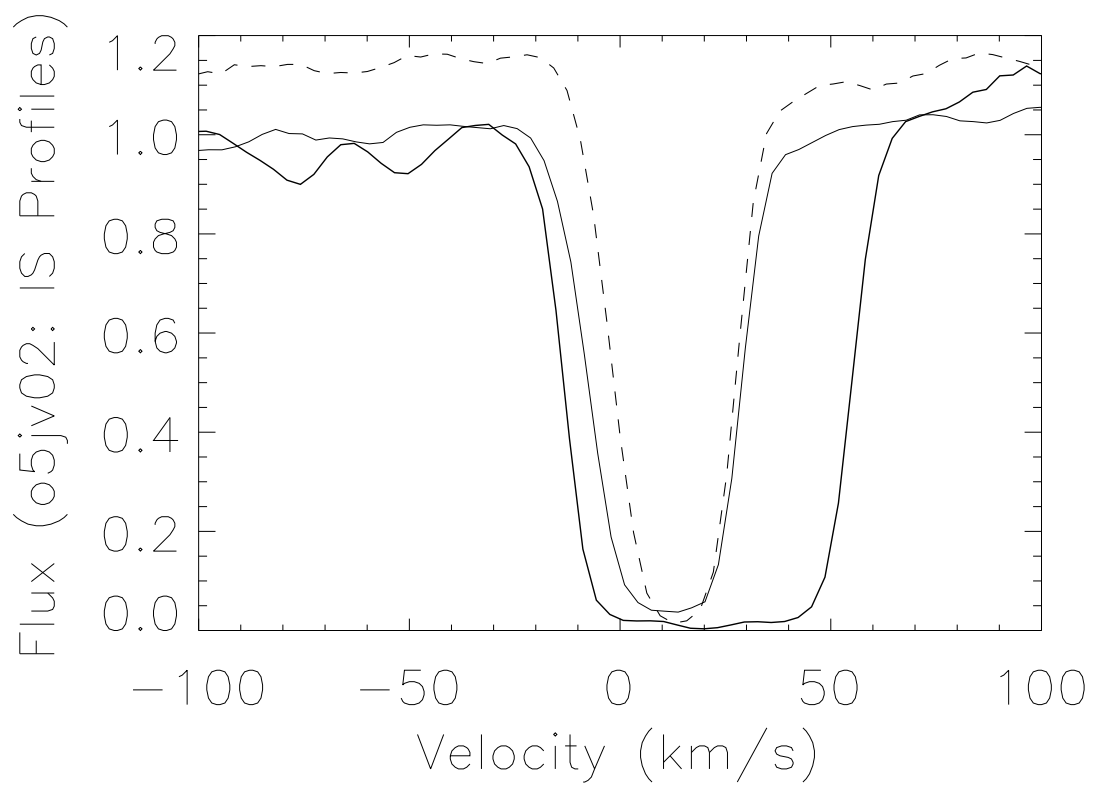


Fig. 10B.— Sample interstellar lines. The solid line shows the two components of the C II 1334, 1335Å doublet, the dashed line is Si II 1260Å.

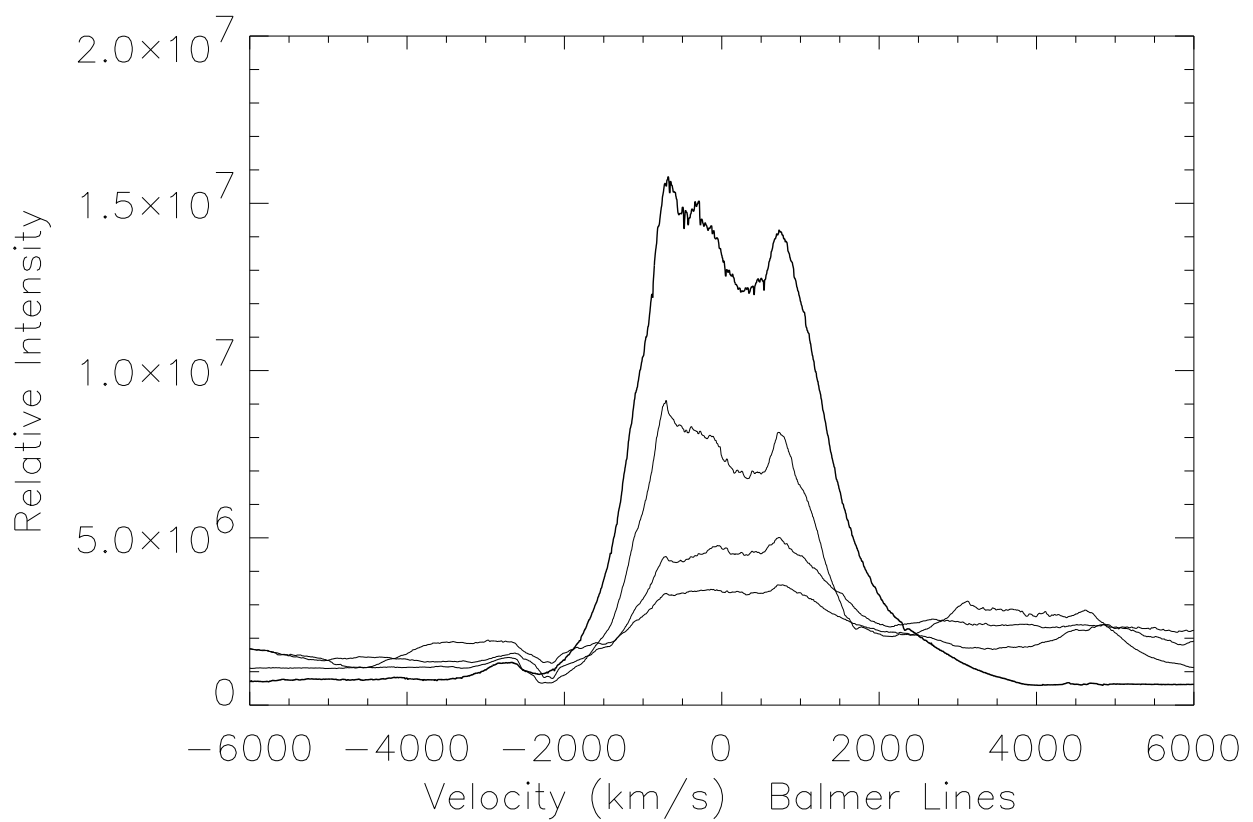


Fig. 11.— ESO spectral line profiles: H α through H δ for V382 Vel (courtesy M. Della Valle)

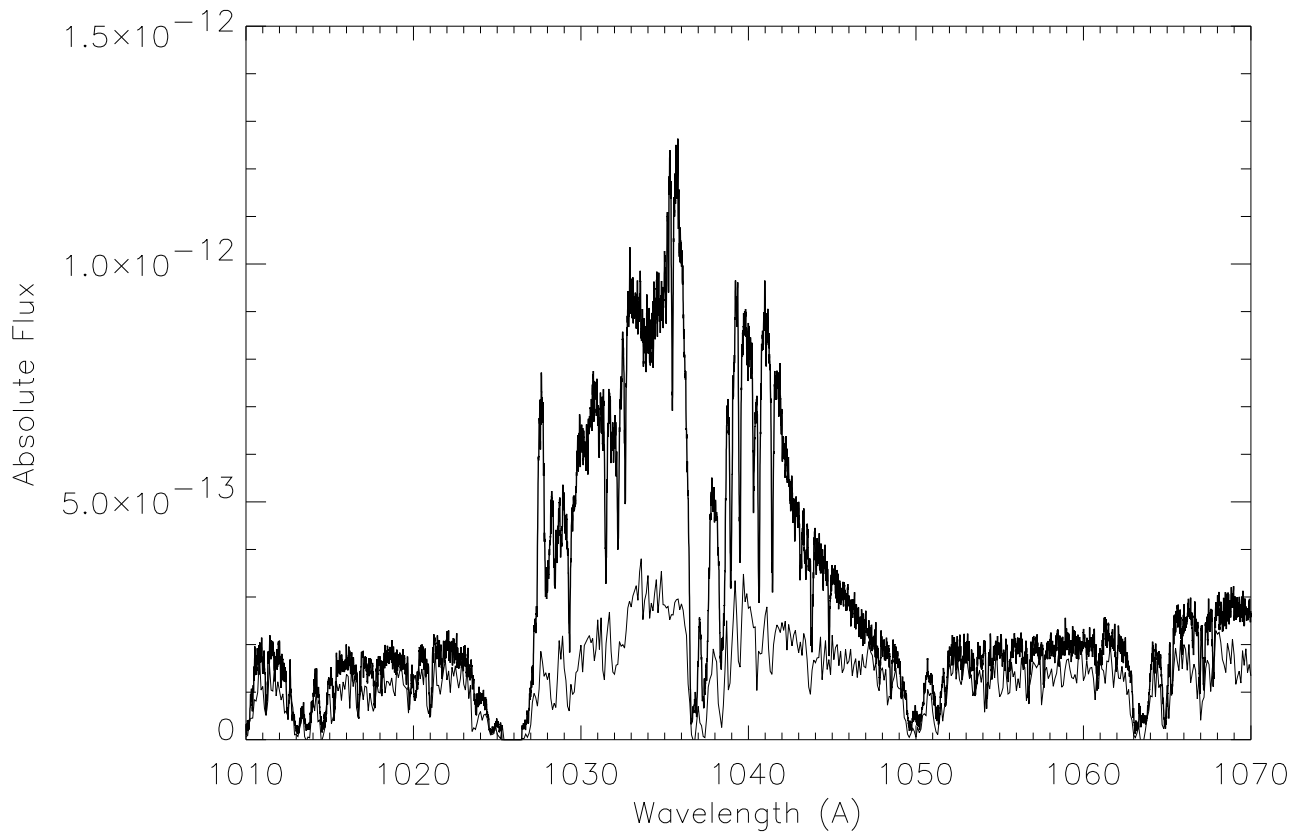


Fig. 12.— Development of O VI 1036Å doublet for V382 Vel in the two FUSE observations (see table 1, 2000 February 6 (thick line), 2000 April 12 (thin line). No reddening corrections have been applied, fluxes are in $\text{erg s}^{-1}\text{cm}^{-2}\text{\AA}^{-1}$.

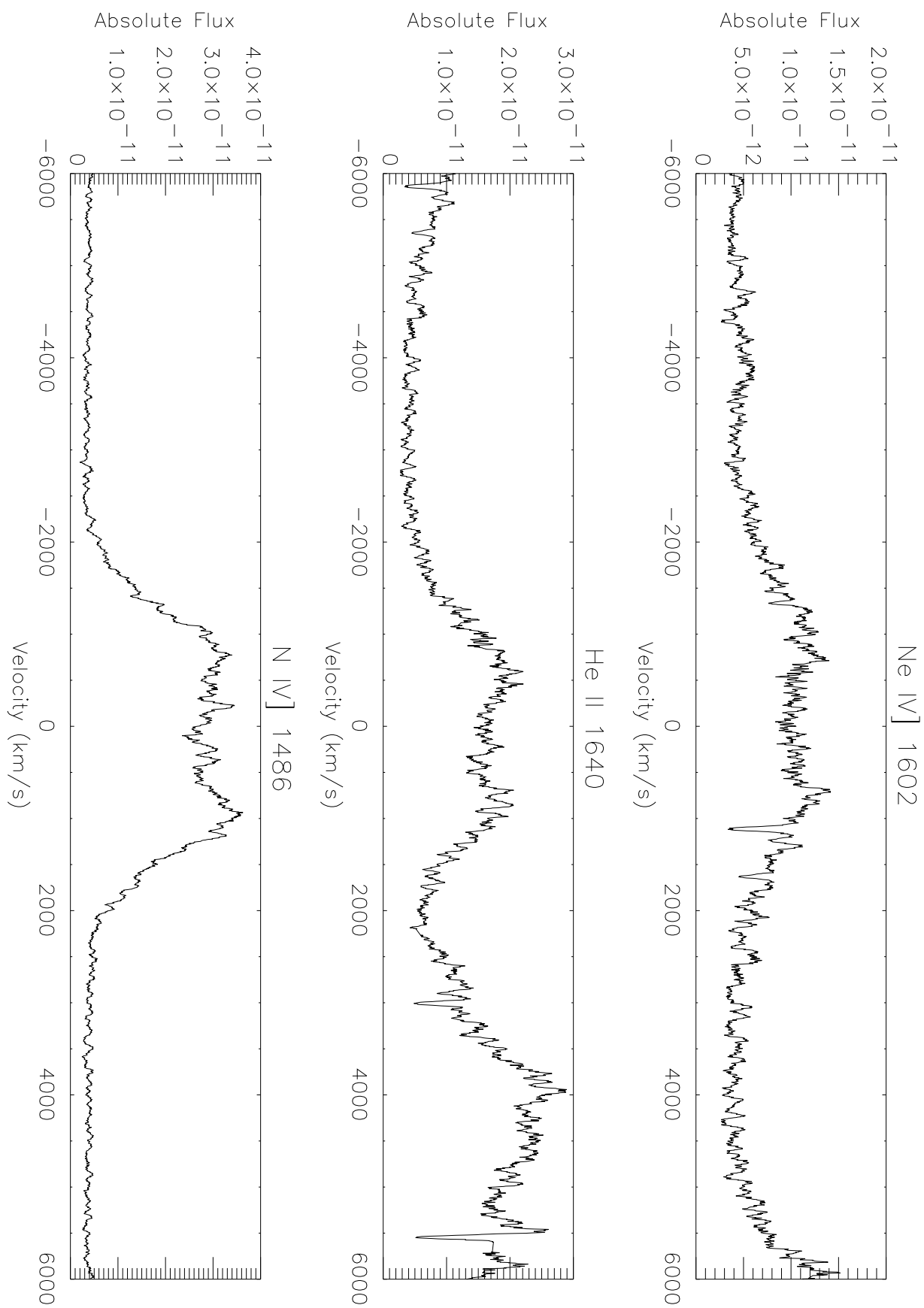


Fig. 13.— Comparison of three emission line profiles for similar ionization transitions of V382 Vel for 1999 August 29.

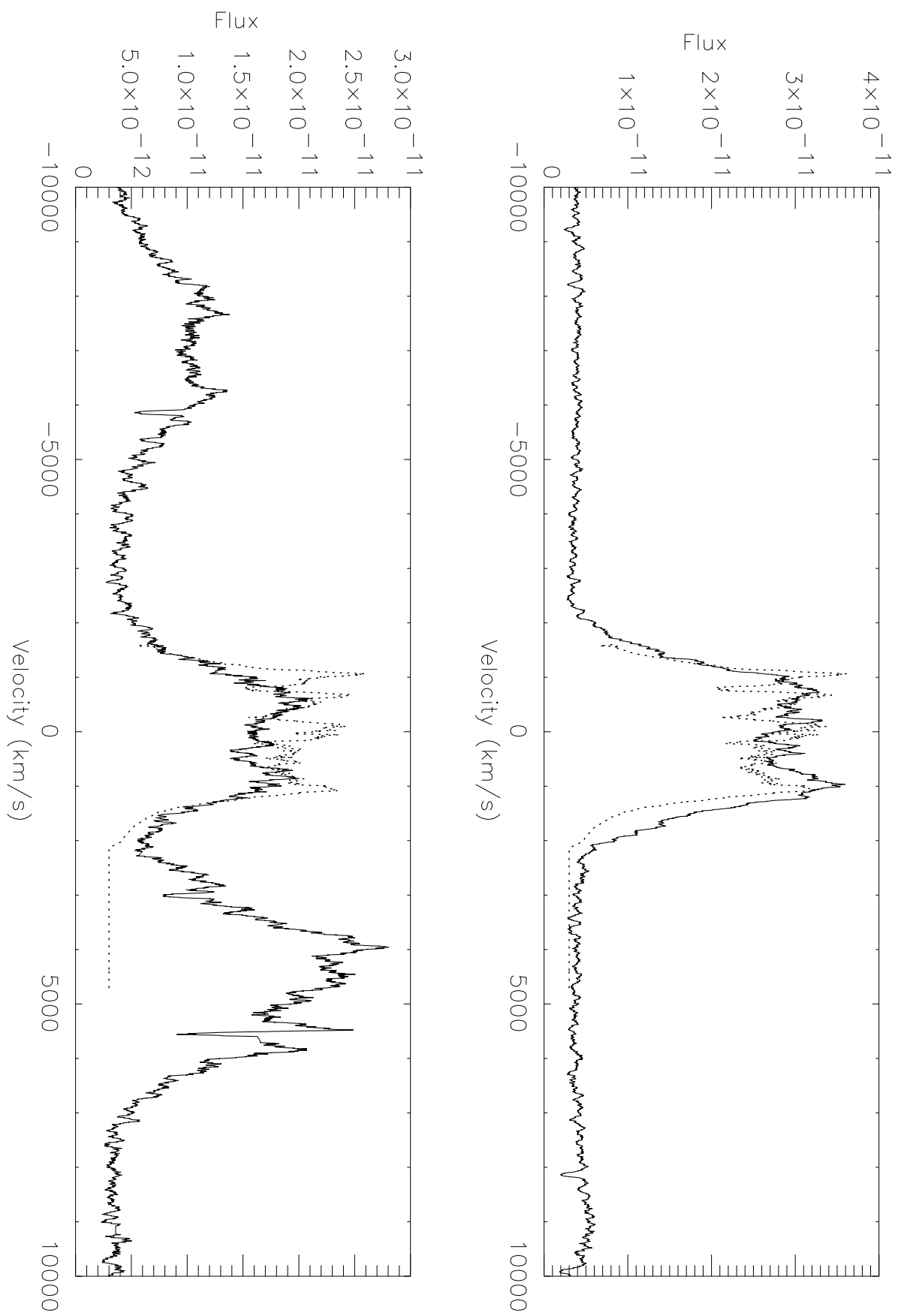


Fig. 14.— Sample ring calculation for $\Delta R/R = 0.5$, for $v_{\max} = 5200 \text{ km s}^{-1}$ for a linear velocity law using a quadratic density dependence for the recombination line emissivity. The top panel shows the spectrum with the 1999 $\Delta v = 61 \text{ km s}^{-1}$ of $\text{N}(\text{IV}) \text{ 1486}\text{\AA}$ the bottom panel shows the

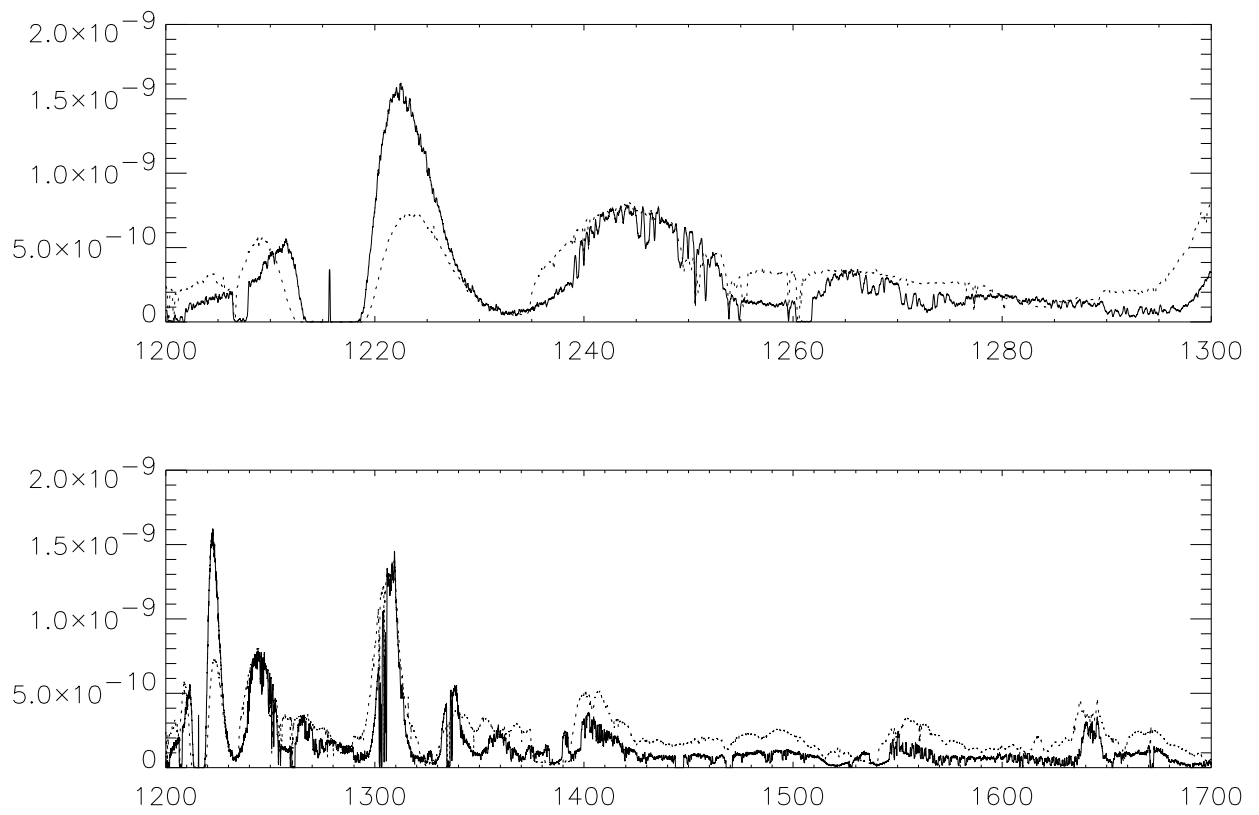


Fig. 15.— Comparison between V382 Vel (dotted line) and Nova LMC 2000 (solid line) at similar stages in outburst, showing both spectral similarities and the effect of different interstellar Ly α absorption on the appearance of the P Cyg component. The emission at Ly α line center is geocoronal

Table 1. Journal of Observations

Instrument	ID	Date (UT)	HJD	Δt^a	Exp (sec)	λ_c (Å)
HST/STIS	O5JV0101	1999 May 31.25	2451330	8	1680	1425
	O5JV0102	1999 May 31.29			1416	1978
	O5JV0103	1999 May 31.33			1100	2707
	O5JV0201	1999 Jun. 21.04	2451351	29	1400	1425
	O5JV0203	1999 Jun. 21.08			1430	1978
	O5JV0204	1999 Jun. 21.14			1100	2707
	O5JV0301	1999 Aug. 29.04	2451420	98	1757	1425
	O5JV0302	1999 Aug. 29.11			2875	1425
	O5JV0303	1999 Aug. 29.18			2842	1978
	O5JV0304	1999 Aug. 29.25			2842	2707
FUSE	A0930201	2000 Feb. 6	2451581	259	92.5×10^3	1060
	A0930202	2000 May 4	2451593	325	11.6×10^3	1060
	A0930203	2000 Jul. 3	2451728	398	25.0×10^3 ^b	1060
	A0930204	2000 Jul. 3	2451728		-	1060

^aTime since visual maximum (1999 May 23.3 UT).

^bCombined exposure time.

Table 2. Emission Line Strengths for STIS Spectrum O5JV03

Species	Wavelength Å	Flux 10^{-10} erg s $^{-1}$ cm $^{-2}$	Notes
N V	1240	3.00	a
O I	1302	1.01	
C II	1335	0.50	
O V	1375	0.13	
Si IV	1400	2.41	
N IV]	1486	3.76	
C IV	1550	2.34	
[Ne IV]	1602	1.17	b
He II	1640	2.07	c
O III]	1667	3.06	
N III]	1750	4.99	
Si II	1816	0.56	
Al III	1860	2.41	
Si III]+C III]	1900	4.37	d
N II	2147	0.42	
C III	2321	0.31	
Al II	2670	2.41	
Mg II	2800	14.3	
O III	3045	0.28	

^aNo extinction corrections have been applied to any quoted fluxes.

^bP Cyg profile, blended with Ly α

^c Upper limit for Ne V] 1575Å is 2×10^{-11} erg s $^{-1}$ cm $^{-2}$; (c) blend on red wing with O III]; (d) F(Si III])/F(C III]) = 0.3.

Table 3. *Cloudy* Emission Line Predictions

Ion	Wavelength (Å)	1st Component ^a (Dense)	2nd Component ^a (Hot)	Total ^a	Observed ^b	χ^2
N V	1240	0.088	0.674	0.762	2.00	6.133
Blend	1400	1.26	3.975
Si IV	1397	0.091	0.019	0.110
O IV	1402	0.263	0.260	0.522
N IV]	1486	1.056	0.854	1.910	1.87	0.438
C IV	1549	0.763	0.436	1.199	1.15	1.023
Ne V]	1575	0.003	0.038	0.042	<0.10	...
Ne IV]	1602	0.146	0.424	0.570	0.57	0.060
He II	1640	0.507 ^c	0.493 ^d	1.000	1.00	0.000
O III]	1665	1.411	0.097	1.507	1.46	0.017
N III]	1750	2.416	0.079	2.495	2.31	0.103
Blend	1810	0.26	1.226
Si II	1808	0.048	0.000	0.048
Ne III	1815	0.127	0.013	0.140
Al III	1860	0.873	0.026	0.899	1.13	0.670
Si III]	1888	0.379	0.005	0.384	0.49	0.754
C III]	1909	1.213	0.030	1.243	1.63	0.903
N II	2140	0.294	0.000	0.295	0.26	0.282
Blend	2324	0.17	2.749
O III	2321	0.070	0.031	0.100
C II	2326	0.140	0.000	0.140
Al II	2665	1.036	0.001	1.037	0.88	0.511
Mg II	2798	4.675	0.030	4.705	4.83	0.011

^aFlux relative to the sum of the two He II fluxes^bDereddened with $E(B - V) = 0.2$ and relative to He II^cHe II Luminosity = 4.3×10^{35} erg s⁻¹^dHe II Luminosity = 4.2×10^{35} erg s⁻¹

Table 4. *Cloudy* Model Parameters

Parameter	Day 110
T_{eff}	1.5×10^5 K
Source luminosity	5×10^{37} erg s $^{-1}$
Hydrogen density	$1.26 \times 10^8, 1.26 \times 10^7$ cm $^{-3}$
Inner radius ^a	2×10^{15} cm
Outer radius ^a	5×10^{15} cm
filling factor	0.05, 0.1
He/He $_{\odot}$ ^b	1.0 (1)
C/C $_{\odot}$ ^b	0.6 (3)
N/N $_{\odot}$ ^b	17 (4)
O/O $_{\odot}$ ^b	3.4 (3)
Ne/Ne $_{\odot}$ ^b	17 (3)
Mg/Mg $_{\odot}$ ^b	2.6 (1)
Al/Al $_{\odot}$ ^b	21 (2)
Si/Si $_{\odot}$ ^b	0.5 (3)

Note. — The first number provided in the density and filling factor rows is from the dense (1st) component while the second number is from the hot (2nd) component. The number in the parentheses in the abundance rows indicates the number of *Cloudy* lines used in the analysis.

^aCalculated assuming a maximum expansion velocity of 5400 km s $^{-1}$ and a ring thickness of 0.5.

^bWhere Log(Solar number abundances relative to hydrogen) He:-1.0 C: -3.45 N: -4.03 O: -3.13 Ne: -3.93 Mg: -4.42 Al: -5.53 Si: -4.45 (Grevesse & Noel 1993).

Table 5. Interstellar Lines: Equivalent Widths

Ion	λ_{lab} (Å)	EW (mÅ)
N I	1199	234
	1200	172
	1201	150
S II	1259	138
Si II	1260	468
P II	1301	38
O I	1302	221
	1304	175
	1306	<3
C II	1334	307
	1335	163
Si IV	1400	9
Si II	1526	236
P II	1533	25
C IV	1548	65
	1550	37
	1671	248
Al II	1854	145
	1863	42
Mg II	2796	575
	2804	510